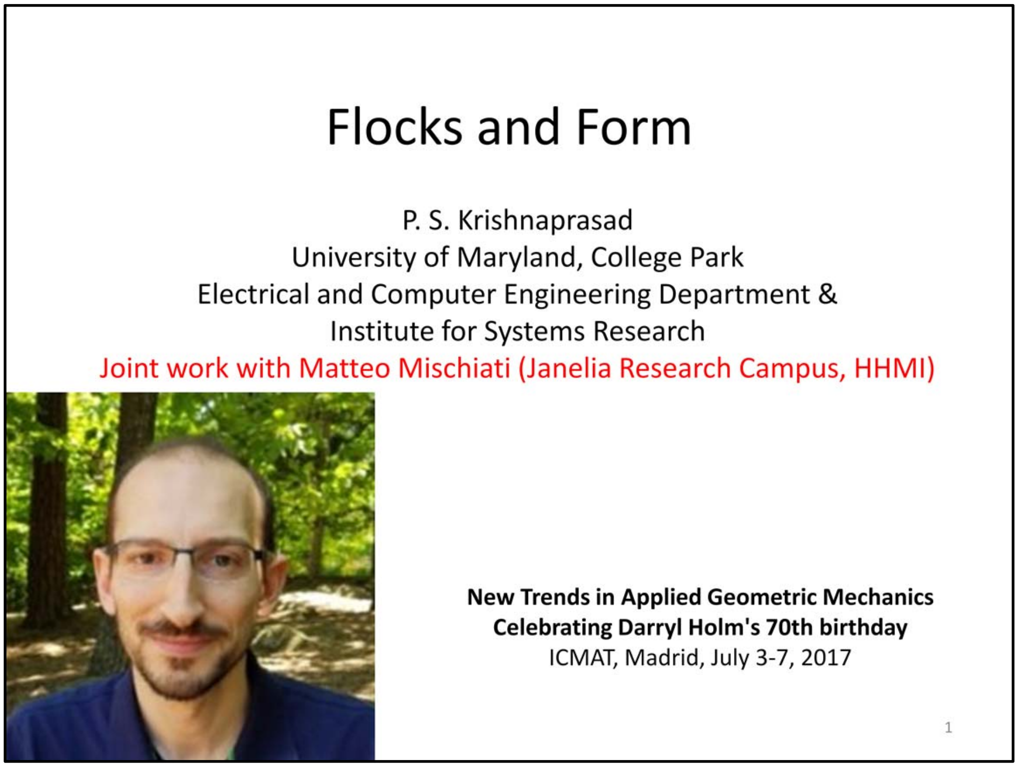

Flocks and Form

P. S. Krishnaprasad
University of Maryland, College Park
Electrical and Computer Engineering Department &
Institute for Systems Research
Joint work with Matteo Mischiati (Janelia Research Campus, HHMI)

New Trends in Applied Geometric Mechanics
Celebrating Darryl Holm's 70th birthday
ICMAT, Madrid, July 3-7, 2017

Collective behavior in nature has attracted attention across a broad spectrum of observers, ranging from artists, biologists, and ecologists, to engineers, mathematicians and physicists. As our ability to gather data in this arena grows, so does the need for refined tools to analyze it with the aim of uncovering the principles and mechanisms of collective motion. In this talk, we present a new construction of a fiber bundle and connection in the sense of Ehresmann, to study such questions. Taken together with the classical notion of principal bundle structure of configuration space over shape space, the results yield ways to decompose collective motion into kinematic modes and to examine associated energy partitions. **This is joint work with Matteo Mischiati**.

Waves of Starlings

FIGURE 3.10 A murmuration of European starlings. Waves of turning in tight flocks of starlings propagate as waves, which are thought to deter predation from birds of prey. *Photo credit: Muffin.*

G. Beauchamp, **Social Predation**, Academic Press, Elsevier Inc., Amsterdam, 2014.

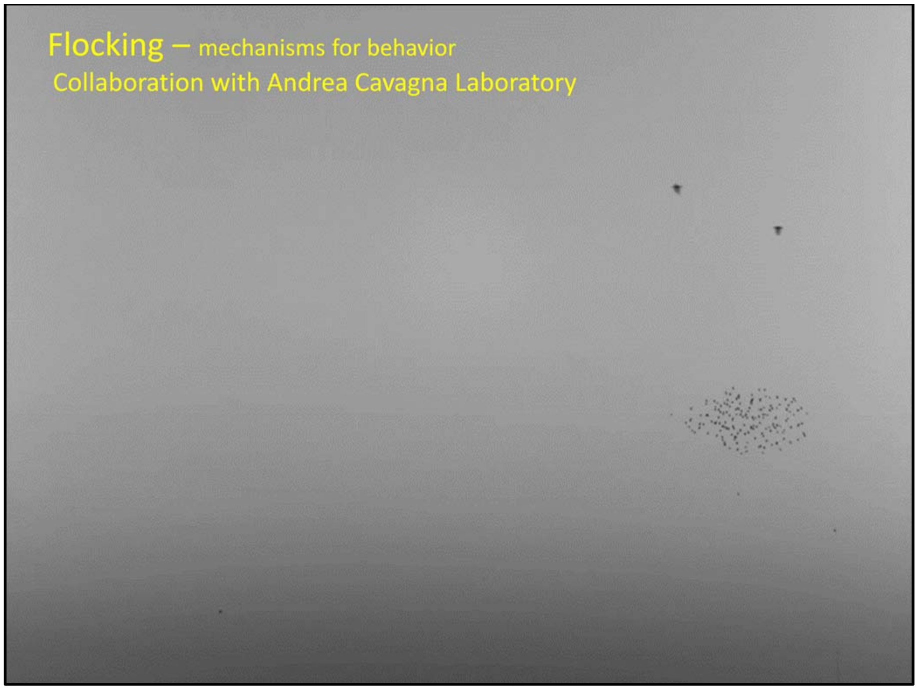
Flocking – mechanisms for behavior
Collaboration with Andrea Cavagna Laboratory

Some Background - In our laboratory at the University of Maryland, we work with trajectory data on flocking behavior of European starlings provided by our collaborator **Dr. Andrea Cavagna** from University of Rome. Our approach aims to uncover the individual-level steering control which gives rise to observed flocking behavior. Here we see a small flock making a cohesive turn, apparently for predator avoidance.

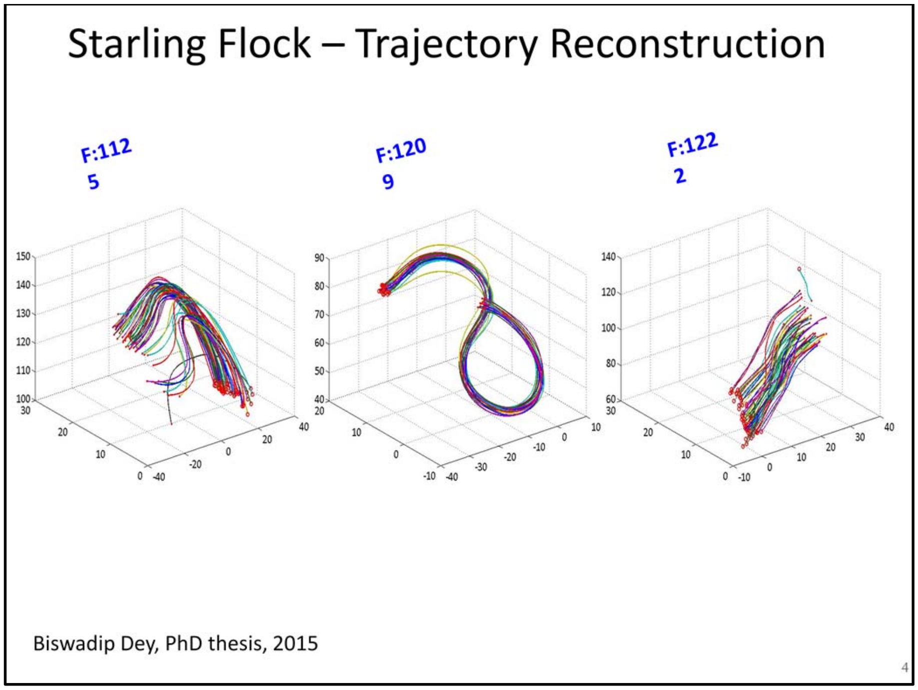

Starling Flock – Trajectory Reconstruction

Biswadip Dey, PhD thesis, 2015

Reconstruction of data, taken from a rooftop spot in the city center of Rome, in front of one of roosting sites used by starlings.

The first event (49) involves a single turn, and the second event (20) involves two consecutive turns. The third event (59) shows a minimally maneuvering flock.

These reconstructions were obtained by applying an optimal control method (with regularizing jerk penalty functional) from sampled data.

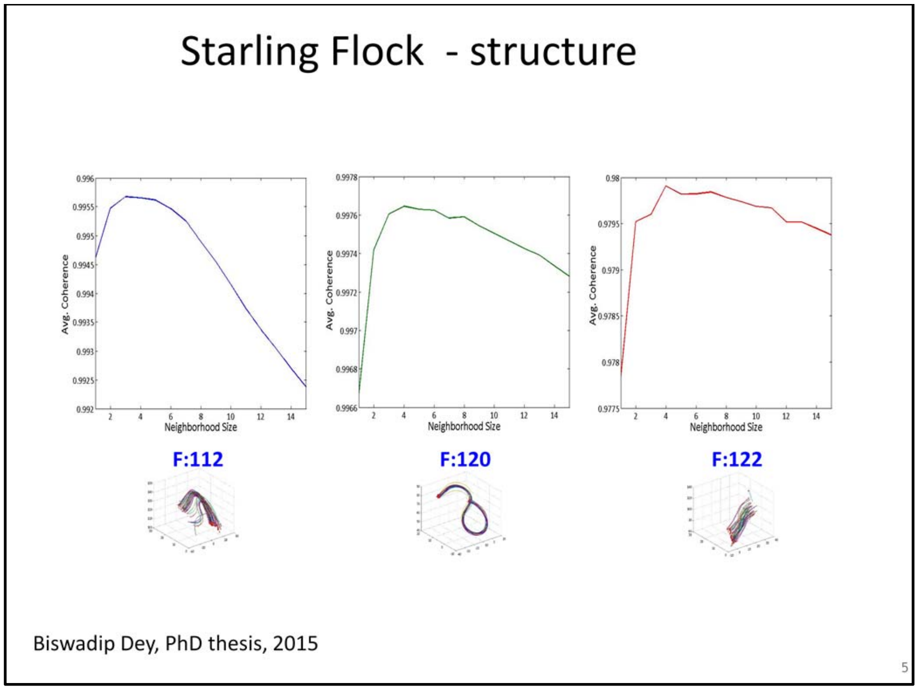

Starling Flock - structure

F:112 **F:120** **F:122**

Biswadip Dey, PhD thesis, 2015

For an individual starling along with its neighborhood (made up k nearest neighbors), define the velocity of the neighborhood center of mass.

The **temporal average value** of the direction cosine between an individual’s velocity and its neighborhood’s center of mass velocity is it’s coherence

The figures show dependence of the **flock-averaged coherence** on the neighborhood size k.

Notice that the dependence on the notion of “k-nearest neighbor” or the topological distance is consistent across different events,

and the flock averaged coherence gets maximized by choosing 5-7 nearest neighbors – earlier noted by Ballerini et. al.

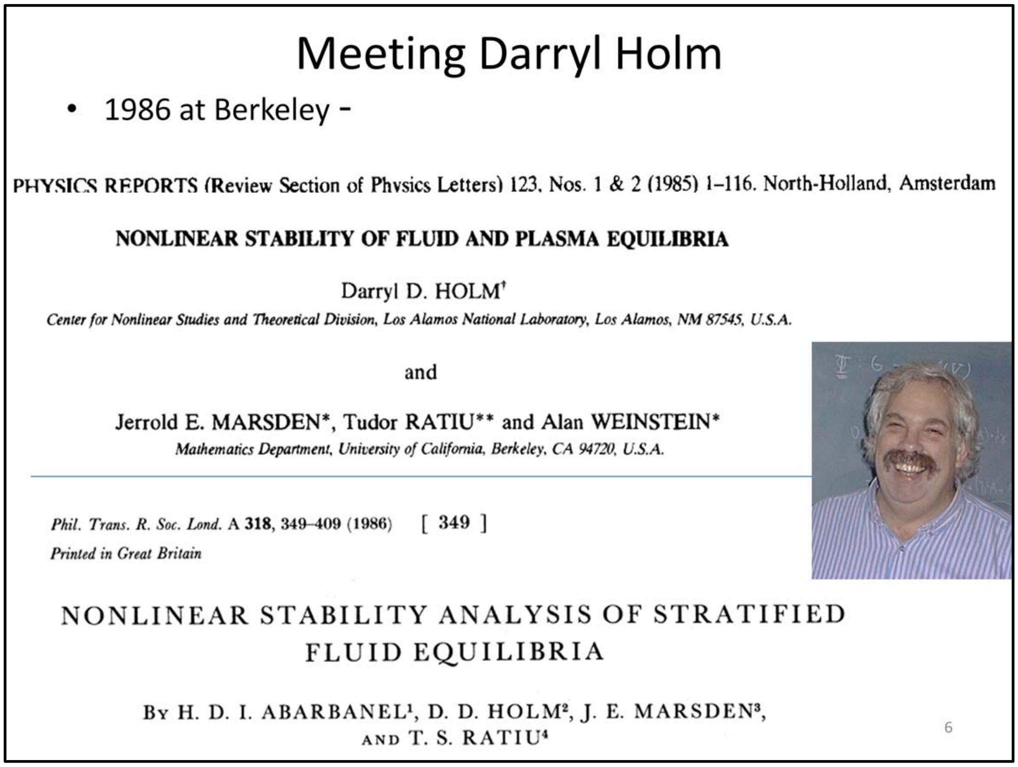

Meeting Darryl Holm

- 1986 at Berkeley -

PHYSICS REPORTS (Review Section of Physics Letters) 123, Nos. 1 & 2 (1985) 1–116. North-Holland, Amsterdam

NONLINEAR STABILITY OF FLUID AND PLASMA EQUILIBRIA

Darryl D. HOLM†
Center for Nonlinear Studies and Theoretical Division, Los Alamos National Laboratory, Los Alamos, NM 87545, U.S.A.

and

Jerrold E. MARSDEN*, Tudor RATIU** and Alan WEINSTEIN*
Mathematics Department, University of California, Berkeley, CA 94720, U.S.A.

Phil. Trans. R. Soc. Lond. A **318**, 349–409 (1986) [**349**]
Printed in Great Britain

NONLINEAR STABILITY ANALYSIS OF STRATIFIED FLUID EQUILIBRIA

By H. D. I. ABARBANEL[1], D. D. HOLM[2], J. E. MARSDEN[3], and T. S. RATIU[4]

6

For me, long before flocks, there were **coupled inert mechanical systems** to think about. Having recently completed work on Lie-Poisson structures associated to coupled rigid bodies, I visited Berkeley at the invitation of Jerrold Marsden in 1984 and was beginning to collaborate on stability questions in mechanics. Soon after, I met Darryl Holm and Tudor Ratiu. Their work on fluid and plasma equilibria were important in my own efforts with Jerry on using the Energy-Casimir method (specifically convexity estimates) to analyze the stability of equilibria of a spinning rigid body with a flexible attachment – a model problem of interest in spacecraft dynamics.

Happy Birthday Darryl

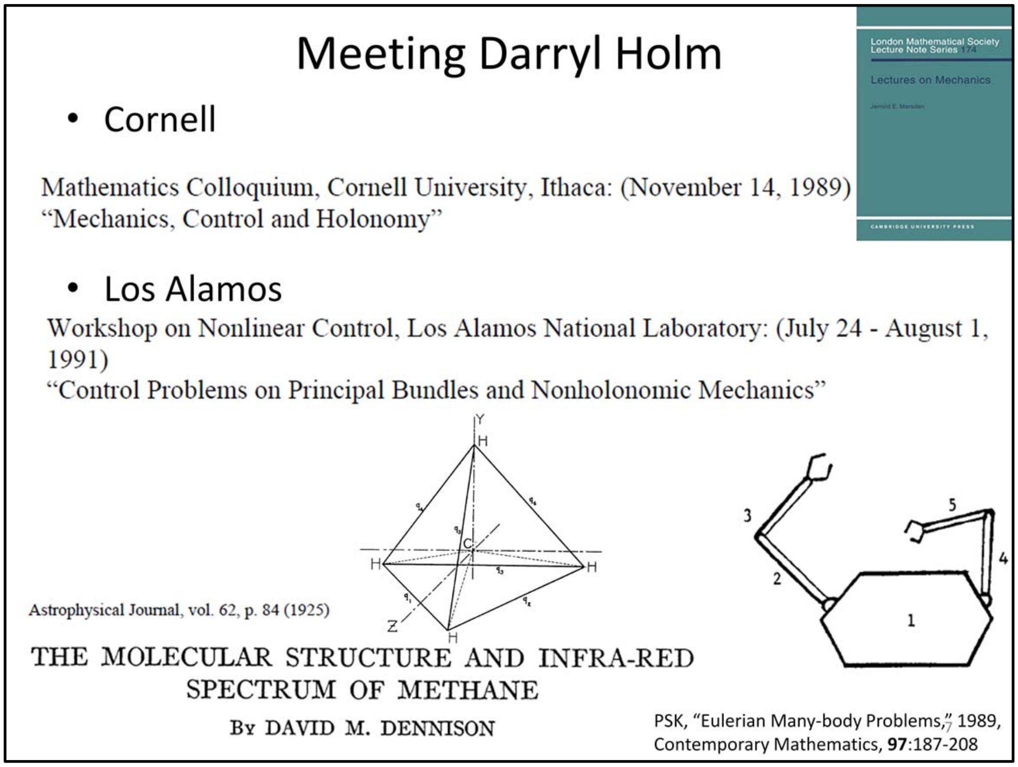

Meeting Darryl Holm

- Cornell

Mathematics Colloquium, Cornell University, Ithaca: (November 14, 1989)
“Mechanics, Control and Holonomy”

- Los Alamos

Workshop on Nonlinear Control, Los Alamos National Laboratory: (July 24 - August 1, 1991)
“Control Problems on Principal Bundles and Nonholonomic Mechanics”

Astrophysical Journal, vol. 62, p. 84 (1925)

THE MOLECULAR STRUCTURE AND INFRA-RED SPECTRUM OF METHANE

BY DAVID M. DENNISON

PSK, “Eulerian Many-body Problems,” 1989, Contemporary Mathematics, **97**:187-208

Soon I became interested in questions of robotics in space, where the problems associated to constraints arising from conservation of angular momentum took center stage. Through interactions with **Richard Montgomery**, I began to appreciate the role of **connections and curvature** in this setting. There was an intense semester (fall 1989) led by **Jerry Marsden** at Cornell which included workshops on geometric phases and related matters. This was a period that also laid the ground work for discussions on links between **geometric mechanics and chemistry** (molecules viewed as many degrees of freedom systems). These things also came up later at a Los Alamos workshop. There is an essential linkage between these subjects. Space robots with joints actuated by motors must respect constraint on overall angular momentum – joint motions couple to overall rotation.

Molecules **vibrate** – infra-red spectroscopy is based on this. They also translate and **rotate**. Can these **normal modes be decoupled?**

No, for reasons of angular momentum constraint. Related questions about discrete symmetry and the ozone molecule were featured in Marsden’s Lectures to the London Mathematical Society (1st edition 1992).

David Dennison, on the Physics faculty at the University of Michigan was a pioneer in the development of a **mechanics of spectroscopy**.

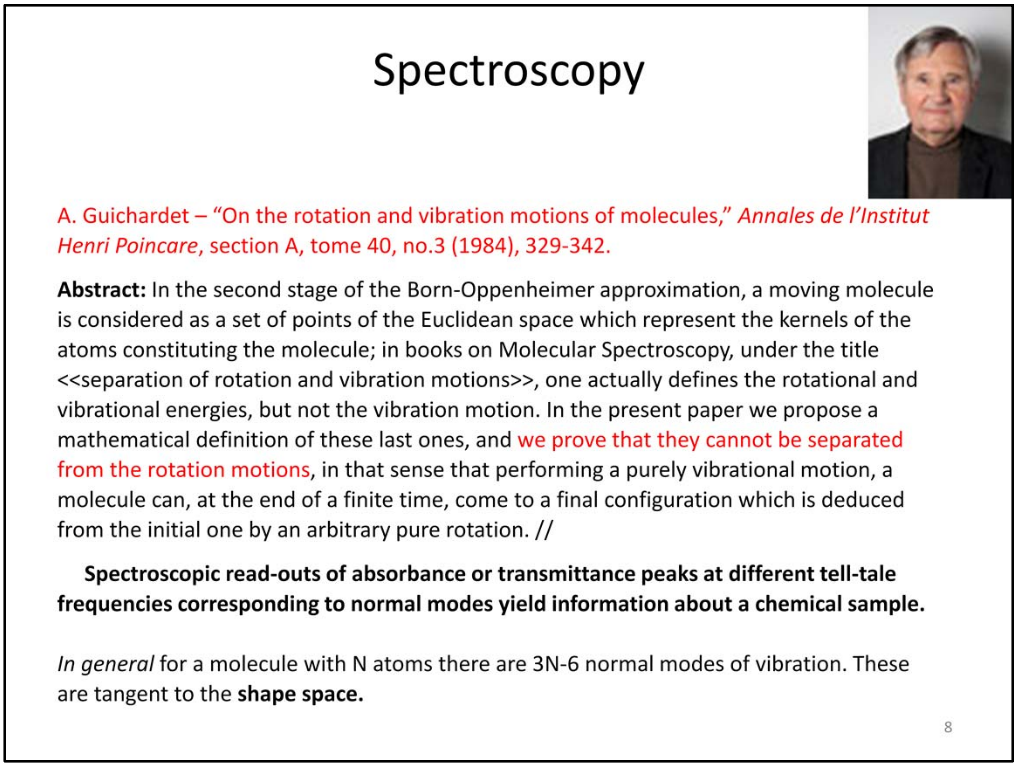

Spectroscopy

A. Guichardet – "On the rotation and vibration motions of molecules," *Annales de l'Institut Henri Poincare*, section A, tome 40, no.3 (1984), 329-342.

Abstract: In the second stage of the Born-Oppenheimer approximation, a moving molecule is considered as a set of points of the Euclidean space which represent the kernels of the atoms constituting the molecule; in books on Molecular Spectroscopy, under the title <<separation of rotation and vibration motions>>, one actually defines the rotational and vibrational energies, but not the vibration motion. In the present paper we propose a mathematical definition of these last ones, and we prove that they cannot be separated from the rotation motions, in that sense that performing a purely vibrational motion, a molecule can, at the end of a finite time, come to a final configuration which is deduced from the initial one by an arbitrary pure rotation. //

Spectroscopic read-outs of absorbance or transmittance peaks at different tell-tale frequencies corresponding to normal modes yield information about a chemical sample.

In general for a molecule with N atoms there are 3N-6 normal modes of vibration. These are tangent to the **shape space.**

8

Guichardet computed the curvature of the (Smale) Guichardet connection on the **principal bundle** of configurations relative to the center of mass with structure group SO(3) and base space = space of shapes. He showed that in general the curvature does not vanish. Thus a **prescribed holonomy** can be realized by a path in the space of shapes, i.e. a sequence of vibrations.

For the space roboticist a related question is how to achieve a prescribed holonomy by an optimal path in joint-space. How much "vibrational cost" must we incur at a minimum for a prescribed overall rotation? **Alex Pines** identified such ISOHOLONOMY problems.

Principle: Operate near the maxima of curvature to get "the most bang for the buck".

These ideas connect with investigations by **Wilczek and Shapere** and others.

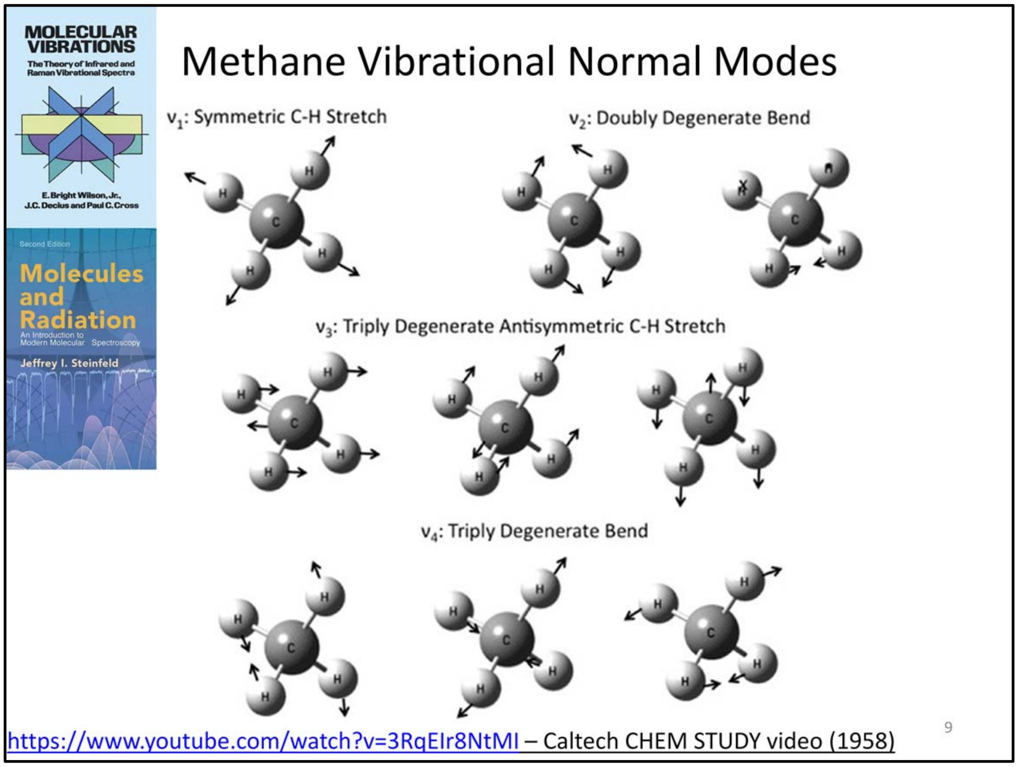

Methane Vibrational Normal Modes

ν_1: Symmetric C-H Stretch

ν_2: Doubly Degenerate Bend

ν_3: Triply Degenerate Antisymmetric C-H Stretch

ν_4: Triply Degenerate Bend

https://www.youtube.com/watch?v=3RqEIr8NtMI – Caltech CHEM STUDY video (1958)

From Physical Chemistry in Action (Figure 18) –

(1) breathing mode – symmetric stretch; (2) doubly degenerate bending mode – same frequencies; (3) triply degenerate antisymmetric stretch; (4) triply degenerate bending mode

Molecules absorb energy from light of a certain frequency (corresponding to a normal mode) and jump to higher level of energy; certain vibrational frequencies are signatures of the presence of certain chemical bonds or functional groups in complex molecules.

Are flocks like complex molecules? When subject to predator attack does a flock display normal modes – or in this talk, kinematic modes?

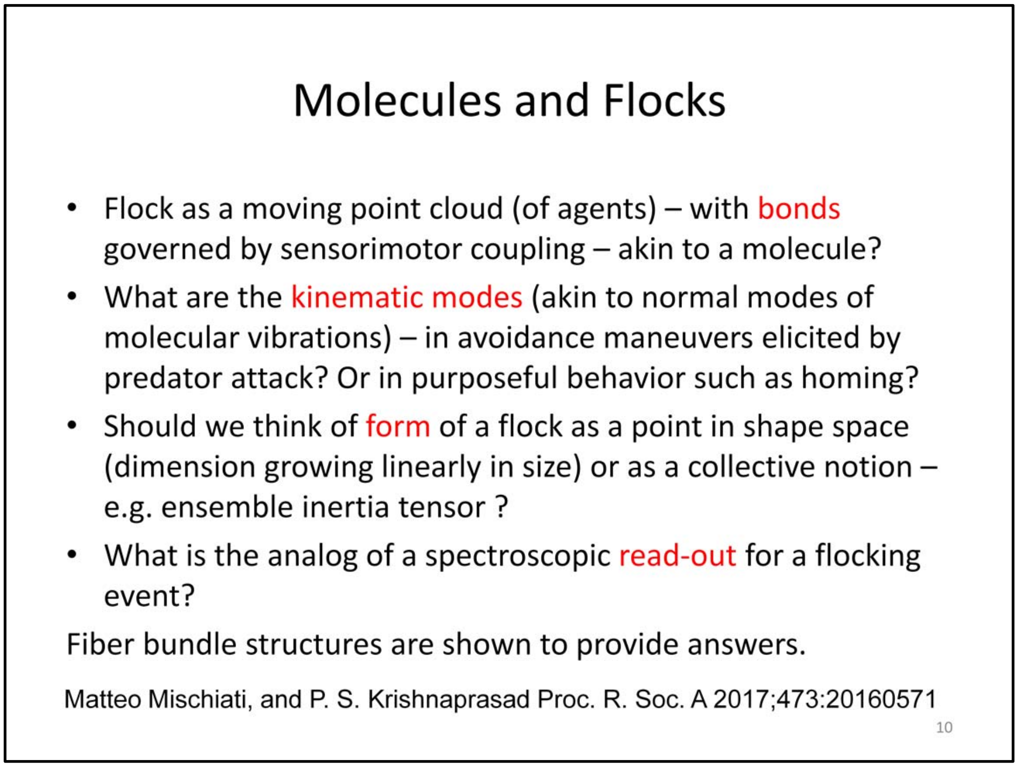

Molecules and Flocks

- Flock as a moving point cloud (of agents) – with bonds governed by sensorimotor coupling – akin to a molecule?
- What are the kinematic modes (akin to normal modes of molecular vibrations) – in avoidance maneuvers elicited by predator attack? Or in purposeful behavior such as homing?
- Should we think of form of a flock as a point in shape space (dimension growing linearly in size) or as a collective notion – e.g. ensemble inertia tensor ?
- What is the analog of a spectroscopic read-out for a flocking event?

Fiber bundle structures are shown to provide answers.

Matteo Mischiati, and P. S. Krishnaprasad Proc. R. Soc. A 2017;473:20160571

Here we pose some questions driven by a loose analogy.
In what follows, we present a top-down view – leading to constructions from data to modes.
This is in contrast to bottom-up synthesis of strategies and feedback laws of interactions, to be tested against raw trajectory data.
Top-down view generates intermediate data representations against which interaction laws can be tested.

Our constructions are built on **fiber bundles**

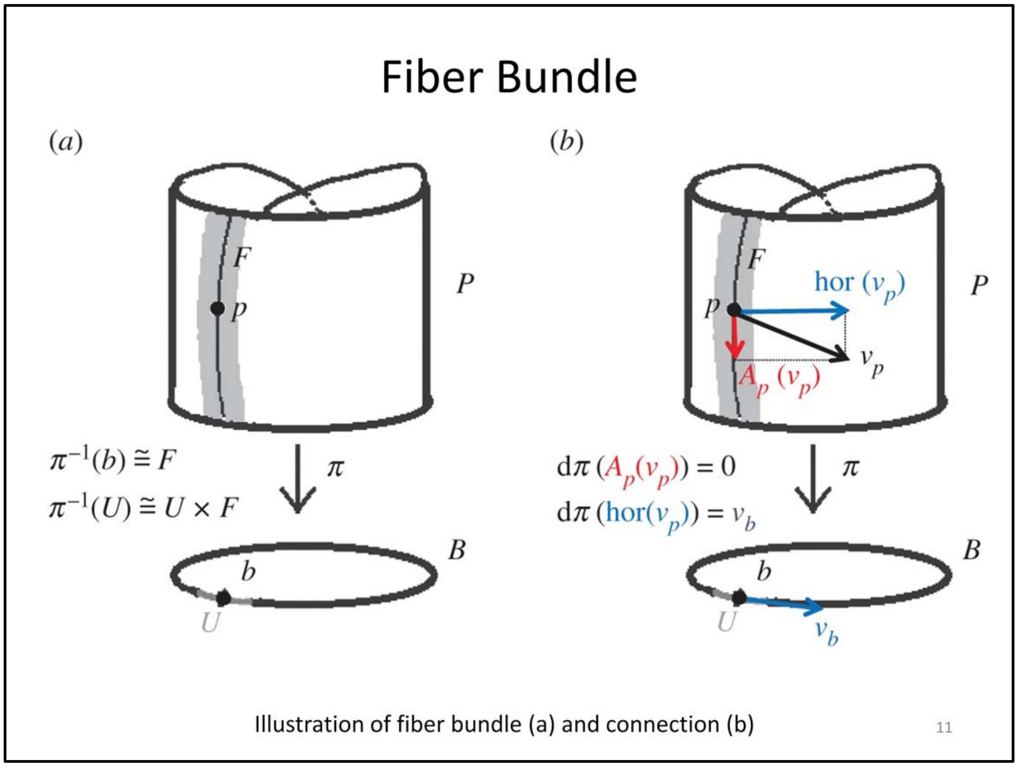

Fiber Bundle

Illustration of fiber bundle (a) and connection (b)

Graphical illustration of (*a*) fiber bundle and (*b*) connection. (*a*) The line passing through $p \in P$ is the fiber over $b = \pi(p)$. The shaded region is $\pi^{-1}(U)$, where U is an open neighbourhood of $b \in B$, which is diffeomorphic to $U \times F$ (a cylinder strip). (*b*) The tangent vector $A_p(v_p)$ along the fiber (vertical) is the one defined by the Ehresmann connection (form) applied to the arbitrary tangent vector v_p (black arrow). The tangent vector hor(v_p) is the other (horizontal) component of v_p, and can be uniquely mapped to a tangent vector v_b on base space through the differential map dπ.

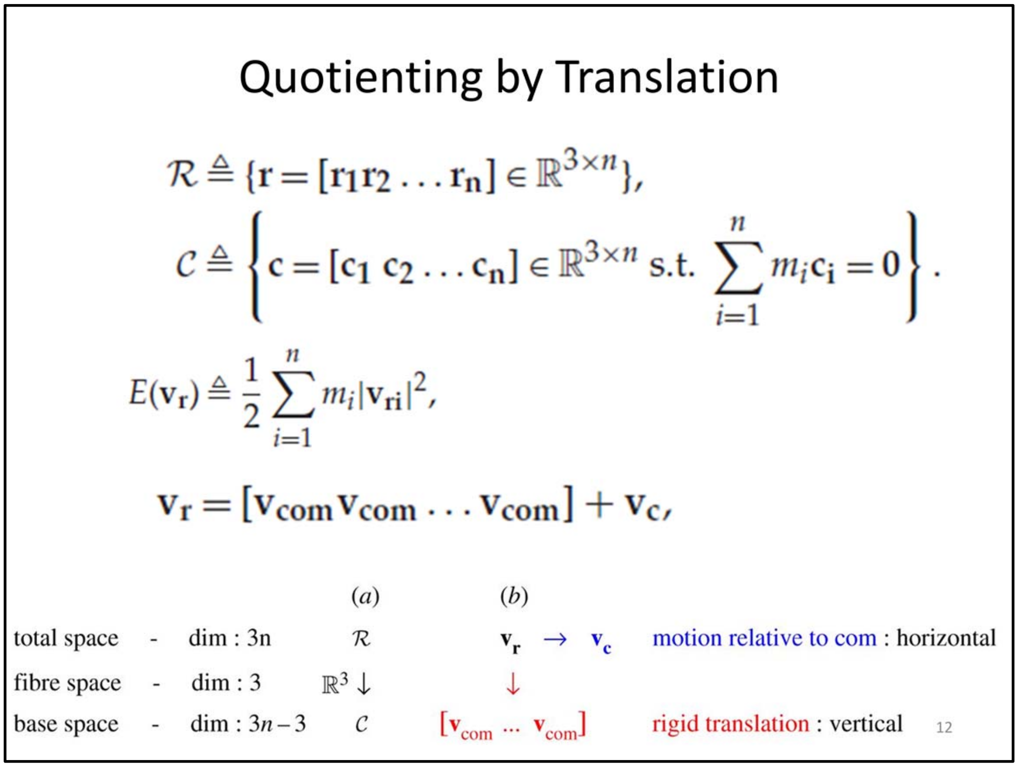

Quotienting by Translation

$$\mathcal{R} \triangleq \{\mathbf{r} = [\mathbf{r}_1 \mathbf{r}_2 \dots \mathbf{r}_\mathbf{n}] \in \mathbb{R}^{3\times n}\},$$

$$\mathcal{C} \triangleq \left\{ \mathbf{c} = [\mathbf{c}_1\ \mathbf{c}_2 \dots \mathbf{c}_\mathbf{n}] \in \mathbb{R}^{3\times n} \text{ s.t. } \sum_{i=1}^{n} m_i \mathbf{c}_\mathbf{i} = 0 \right\}.$$

$$E(\mathbf{v}_\mathbf{r}) \triangleq \frac{1}{2} \sum_{i=1}^{n} m_i |\mathbf{v}_{\mathbf{ri}}|^2,$$

$$\mathbf{v}_\mathbf{r} = [\mathbf{v}_{\mathbf{com}} \mathbf{v}_{\mathbf{com}} \dots \mathbf{v}_{\mathbf{com}}] + \mathbf{v}_\mathbf{c},$$

			(*a*)	(*b*)	
total space	-	dim : 3n	$\mathcal{R}$	$\mathbf{v}_\mathbf{r} \rightarrow \mathbf{v}_\mathbf{c}$	motion relative to com : horizontal
fibre space	-	dim : 3	$\mathbb{R}^3 \downarrow$	$\downarrow$	
base space	-	dim : $3n-3$	$\mathcal{C}$	$[\mathbf{v}_{\text{com}} \dots \mathbf{v}_{\text{com}}]$	rigid translation : vertical

We proceed to construct fiber bundles from the space of point clouds. Schematic of (*a*) rigid translation fibering and (*b*) the associated orthogonal decomposition of an arbitrary collective motion vr∈TrR.

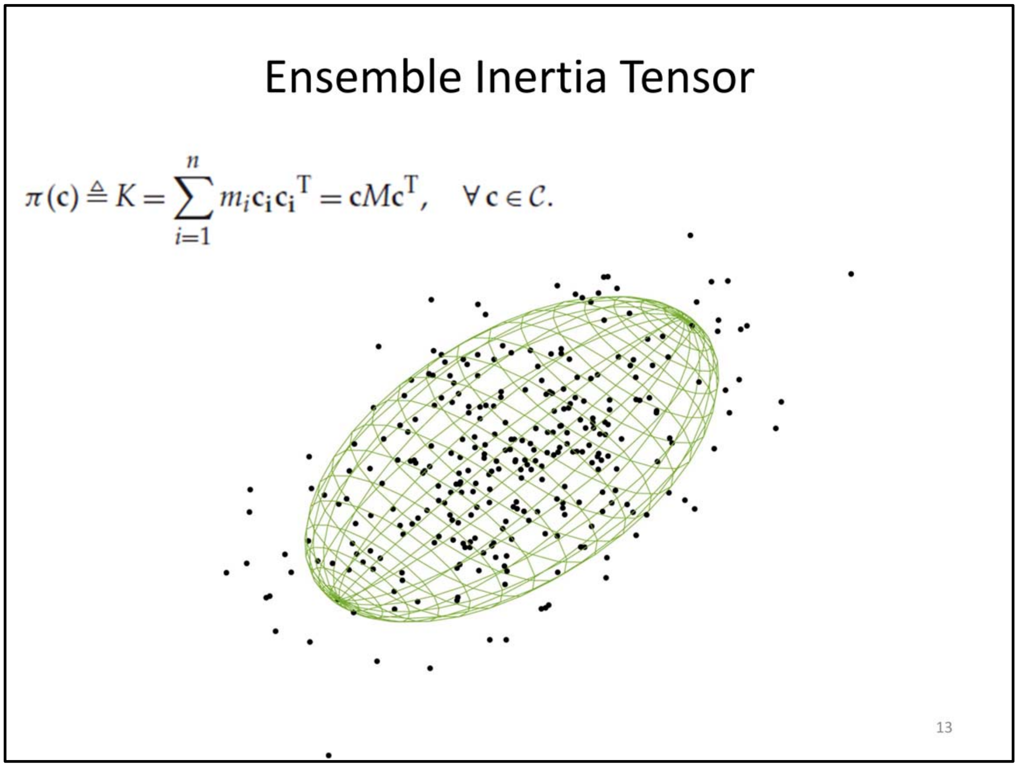

Ensemble Inertia Tensor

$$\pi(\mathbf{c}) \triangleq K = \sum_{i=1}^{n} m_i \mathbf{c_i}\mathbf{c_i}^{\mathrm{T}} = \mathbf{c}M\mathbf{c}^{\mathrm{T}}, \quad \forall\, \mathbf{c} \in \mathcal{C}.$$

The **ensemble inertia tensor *K*** of a collective can be visualized as an ellipsoid centered at the center of mass, with semi-principal axes of length proportional to the eigenvalues of *K* and pointing in the direction of the corresponding eigenvectors.

Any configuration relative to center of mass (i.e. point cloud) also defines a **polygon**. Thus here we pass from a polygon to an **ellipsoid**.

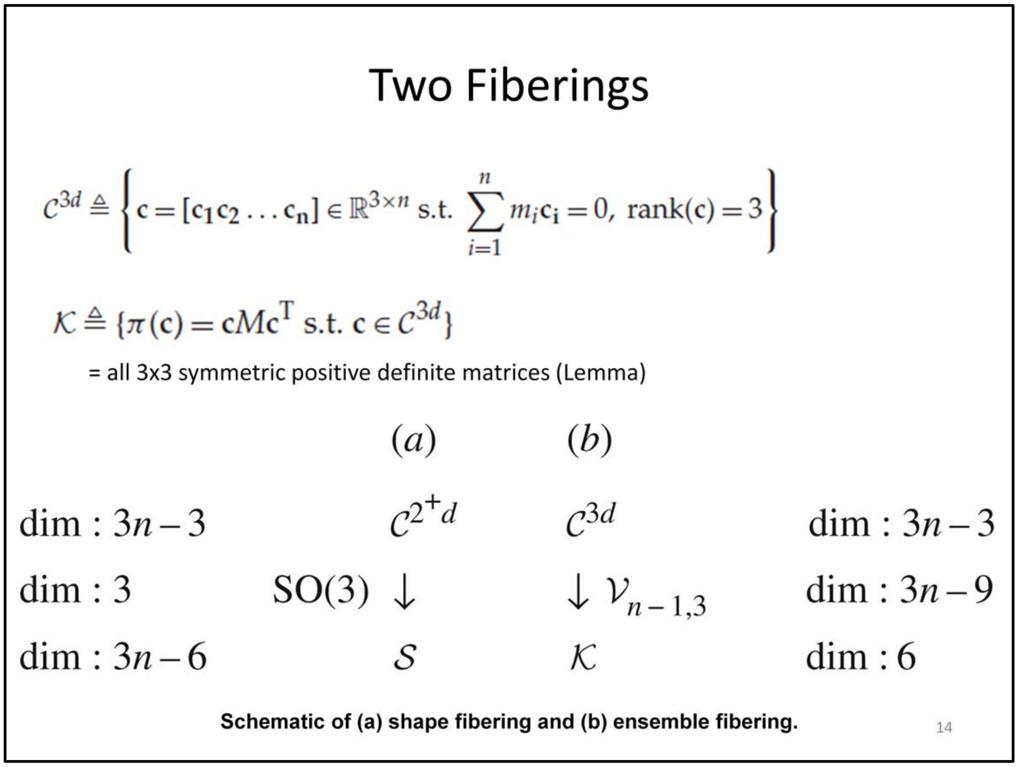

Two Fiberings

$$\mathcal{C}^{3d} \triangleq \left\{ \mathbf{c} = [\mathbf{c_1 c_2} \ldots \mathbf{c_n}] \in \mathbb{R}^{3\times n} \text{ s.t. } \sum_{i=1}^{n} m_i \mathbf{c_i} = 0,\ \operatorname{rank}(\mathbf{c}) = 3 \right\}$$

$$\mathcal{K} \triangleq \{\pi(\mathbf{c}) = \mathbf{c} M \mathbf{c}^{\mathrm{T}} \text{ s.t. } \mathbf{c} \in \mathcal{C}^{3d}\}$$

= all 3x3 symmetric positive definite matrices (Lemma)

$$\begin{tikzcd}
 & (a) & (b) & \\
\dim: 3n-3 & \mathcal{C}^{2^+d} \arrow[dd, "\mathrm{SO}(3)"'] & \mathcal{C}^{3d} \arrow[dd, "\mathcal{V}_{n-1,3}"] & \dim: 3n-3 \\
\dim: 3 & & & \dim: 3n-9 \\
\dim: 3n-6 & \mathcal{S} & \mathcal{K} & \dim: 6
\end{tikzcd}$$

Schematic of (a) shape fibering and (b) ensemble fibering.

Schematic of (a) shape fibering with structure group SO(3) and (b) ensemble fibering with fiber **Stiefel manifold** of (n-1)x3 orthonormal matrices

Fibers

Ensemble fibering has fibers diffeomorphic to Stiefel manifold

$$\mathcal{V}_{n-1,3} \triangleq \{V \in \mathbb{R}^{(n-1)\times 3} \text{ s.t. } V^{\mathrm{T}}V = \mathbb{1}\}$$

with diffeomorphism given by

$$f_{K,W}:\ \mathbf{c} \in \pi^{-1}(K) \mapsto V = f_{K,W}(\mathbf{c}) = W^{\mathrm{T}}M^{1/2}\mathbf{c}^{\mathrm{T}}Q^{\mathrm{T}}\Lambda^{-1/2} \in \mathcal{V}_{n-1,3}$$

where W is any $n \times (n-1)$ matrix with orthonormal columns orthogonal to the vector $[\sqrt{m_1/m_{\mathrm{tot}}} \cdots \sqrt{m_n/m_{\mathrm{tot}}}]^{\mathrm{T}}$.

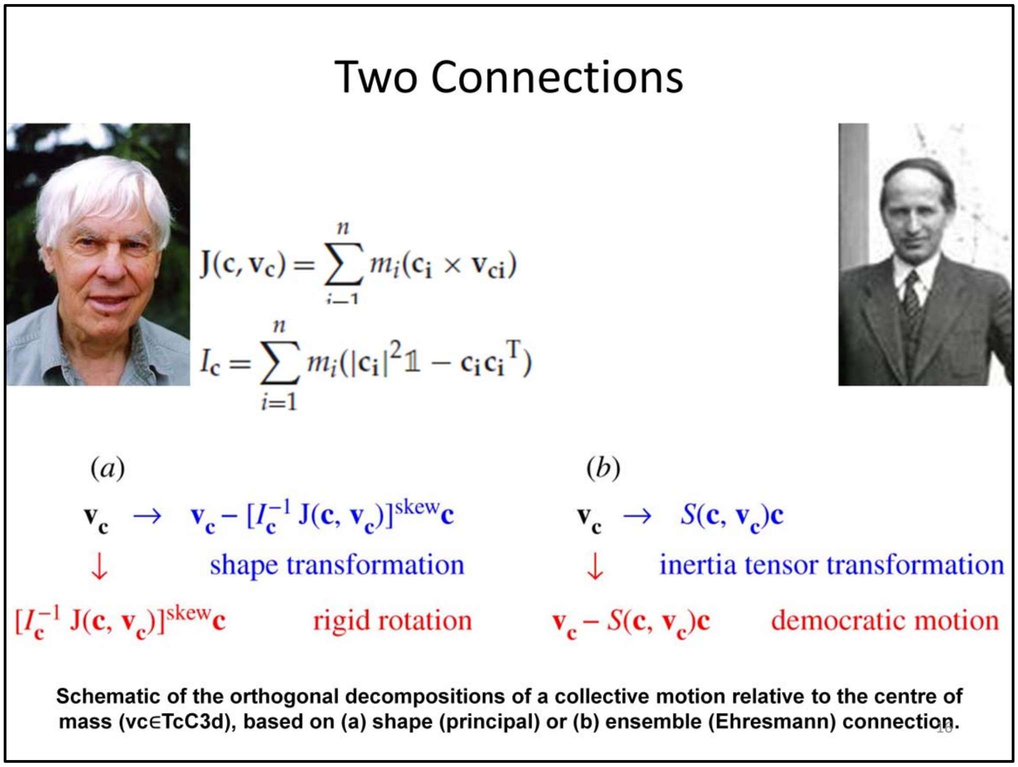

Two Connections

$$\mathrm{J}(\mathbf{c}, \mathbf{v_c}) = \sum_{i—1}^{n} m_i(\mathbf{c_i} \times \mathbf{v_{ci}})$$

$$I_{\mathbf{c}} = \sum_{i=1}^{n} m_i(|\mathbf{c_i}|^2 \mathbb{1} - \mathbf{c_i}\mathbf{c_i}^{\mathrm{T}})$$

(*a*)

$\mathbf{v_c} \rightarrow \mathbf{v_c} - [I_{\mathbf{c}}^{-1}\, \mathrm{J}(\mathbf{c}, \mathbf{v_c})]^{\mathrm{skew}}\mathbf{c}$

$\downarrow$ shape transformation

$[I_{\mathbf{c}}^{-1}\, \mathrm{J}(\mathbf{c}, \mathbf{v_c})]^{\mathrm{skew}}\mathbf{c}$ rigid rotation

(*b*)

$\mathbf{v_c} \rightarrow S(\mathbf{c}, \mathbf{v_c})\mathbf{c}$

$\downarrow$ inertia tensor transformation

$\mathbf{v_c} - S(\mathbf{c}, \mathbf{v_c})\mathbf{c}$ democratic motion

Schematic of the orthogonal decompositions of a collective motion relative to the centre of mass (vc∈TcC3d), based on (a) shape (principal) or (b) ensemble (Ehresmann) connection.

Schematic of the orthogonal decompositions of a collective motion relative to the center of mass (vc ∈ TcC3d), based on (*a*) shape or (*b*) ensemble connection.

Lyapunov and Ehresmann

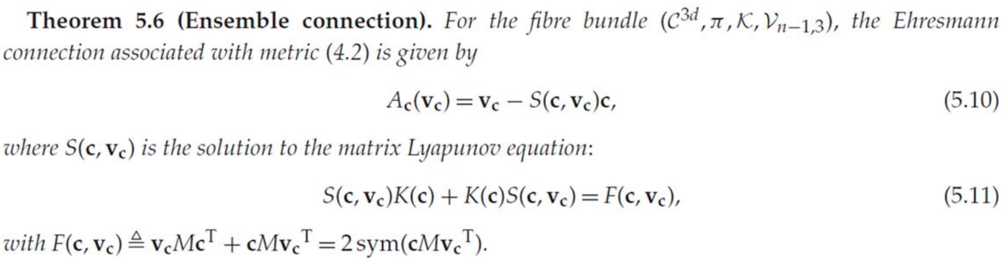

Theorem 5.6 (Ensemble connection). *For the fibre bundle* $(\mathcal{C}^{3d}, \pi, \mathcal{K}, \mathcal{V}_{n-1,3})$, *the Ehresmann connection associated with metric* (4.2) *is given by*

$$A_{\mathbf{c}}(\mathbf{v}_{\mathbf{c}}) = \mathbf{v}_{\mathbf{c}} - S(\mathbf{c}, \mathbf{v}_{\mathbf{c}})\mathbf{c}, \tag{5.10}$$

where $S(\mathbf{c}, \mathbf{v}_{\mathbf{c}})$ *is the solution to the matrix Lyapunov equation*:

$$S(\mathbf{c}, \mathbf{v}_{\mathbf{c}})K(\mathbf{c}) + K(\mathbf{c})S(\mathbf{c}, \mathbf{v}_{\mathbf{c}}) = F(\mathbf{c}, \mathbf{v}_{\mathbf{c}}), \tag{5.11}$$

with $F(\mathbf{c}, \mathbf{v}_{\mathbf{c}}) \triangleq \mathbf{v}_{\mathbf{c}} M \mathbf{c}^{\mathrm{T}} + \mathbf{c} M {\mathbf{v}_{\mathbf{c}}}^{\mathrm{T}} = 2\,\mathrm{sym}(\mathbf{c} M {\mathbf{v}_{\mathbf{c}}}^{\mathrm{T}})$.

Matteo Mischiati, and P. S. Krishnaprasad Proc. R. Soc. A 2017;473:20160571

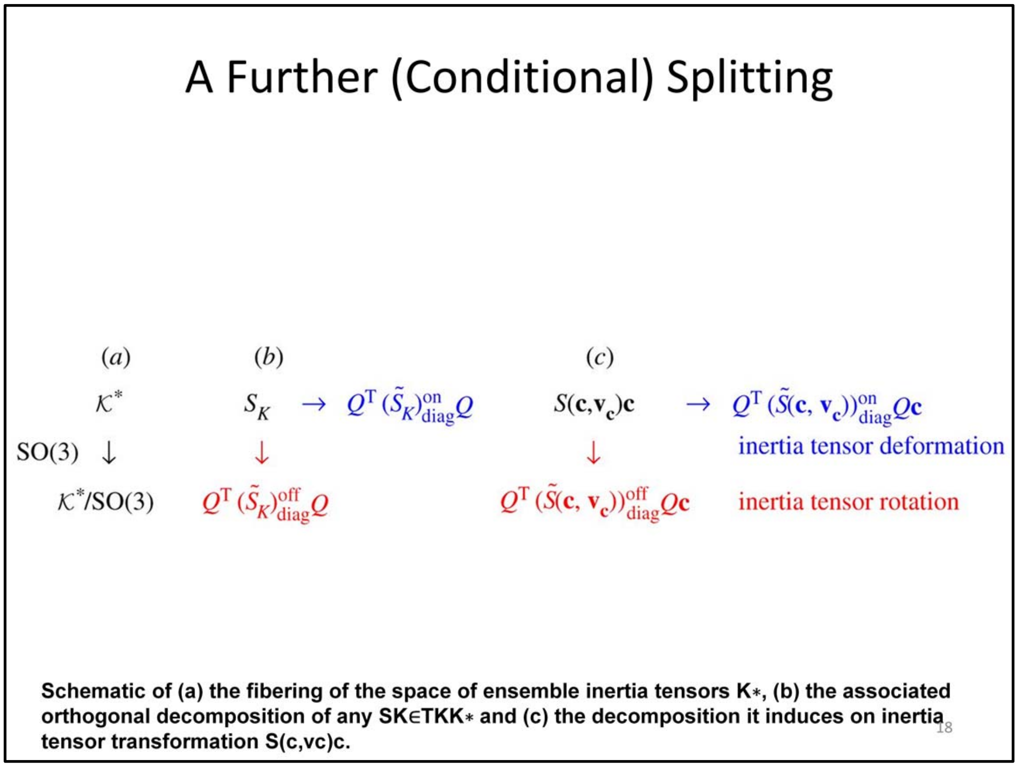

A Further (Conditional) Splitting

$$\begin{tikzcd}
(a) & (b) & & (c) & & \\
\mathcal{K}^* \arrow[d, "\mathrm{SO}(3)"'] & S_K \arrow[r] \arrow[d] & Q^{\mathrm{T}}\,(\tilde{S}_K)^{\mathrm{on}}_{\mathrm{diag}}Q & S(\mathbf{c},\mathbf{v_c})\mathbf{c} \arrow[r] \arrow[d] & Q^{\mathrm{T}}\,(\tilde{S}(\mathbf{c},\,\mathbf{v_c}))^{\mathrm{on}}_{\mathrm{diag}}Q\mathbf{c} & \text{inertia tensor deformation} \\
\mathcal{K}^*/\mathrm{SO}(3) & Q^{\mathrm{T}}\,(\tilde{S}_K)^{\mathrm{off}}_{\mathrm{diag}}Q & & Q^{\mathrm{T}}\,(\tilde{S}(\mathbf{c},\,\mathbf{v_c}))^{\mathrm{off}}_{\mathrm{diag}}Q\mathbf{c} & & \text{inertia tensor rotation}
\end{tikzcd}$$

Schematic of (a) the fibering of the space of ensemble inertia tensors K∗, (b) the associated orthogonal decomposition of any SK∈TKK∗ and (c) the decomposition it induces on inertia tensor transformation S(c,vc)c.

Schematic of (*a*) the fibering of the space of ensemble inertia tensors K∗, (*b*) the associated orthogonal decomposition of any SK∈TKK∗ and (*c*) the decomposition it induces on inertia tensor transformation $S(\mathbf{c},\mathbf{v_c})\mathbf{c}$.

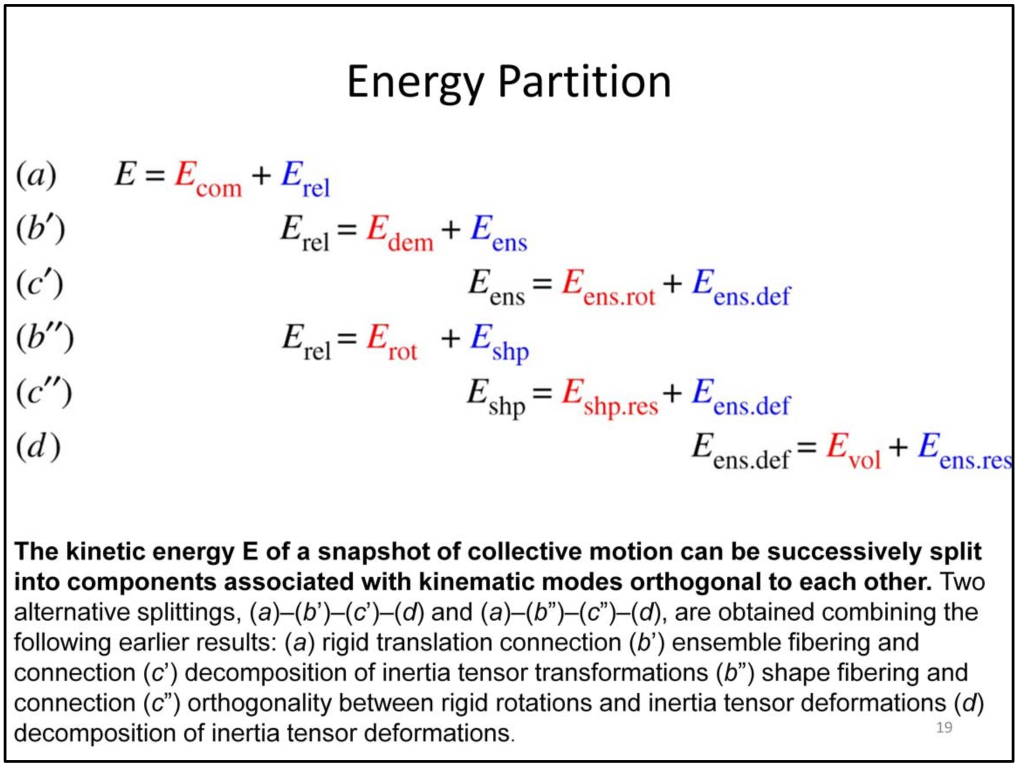

Energy Partition

$$
\begin{array}{ll}
(a) & E = E_{\text{com}} + E_{\text{rel}} \\
(b') & E_{\text{rel}} = E_{\text{dem}} + E_{\text{ens}} \\
(c') & E_{\text{ens}} = E_{\text{ens.rot}} + E_{\text{ens.def}} \\
(b'') & E_{\text{rel}} = E_{\text{rot}} + E_{\text{shp}} \\
(c'') & E_{\text{shp}} = E_{\text{shp.res}} + E_{\text{ens.def}} \\
(d) & E_{\text{ens.def}} = E_{\text{vol}} + E_{\text{ens.res}}
\end{array}
$$

The kinetic energy E of a snapshot of collective motion can be successively split into components associated with kinematic modes orthogonal to each other. Two alternative splittings, (*a*)–(*b*')–(*c*')–(*d*) and (*a*)–(*b*")–(*c*")–(*d*), are obtained combining the following earlier results: (*a*) rigid translation connection (*b*') ensemble fibering and connection (*c*') decomposition of inertia tensor transformations (*b*") shape fibering and connection (*c*") orthogonality between rigid rotations and inertia tensor deformations (*d*) decomposition of inertia tensor deformations.

The kinetic energy $E(\mathbf{v}_r)$ of a snapshot of collective motion vr ∈ TrR can be iteratively split into additive components associated with elementary motions orthogonal to each other. Two alternative splittings, (*a*)–(*b*')–(*c*')–(*d*) and (*a*)–(*b*")–(*c*")–(*d*), are obtained combining the following earlier results: (*a*) rigid translation connection (*b*') ensemble fibering and connection (*c*') decomposition of inertia tensor transformations (*b*") shape fibering and connection (*c*") orthogonality between rigid rotations and inertia tensor deformations (*d*) decomposition of inertia tensor deformations.

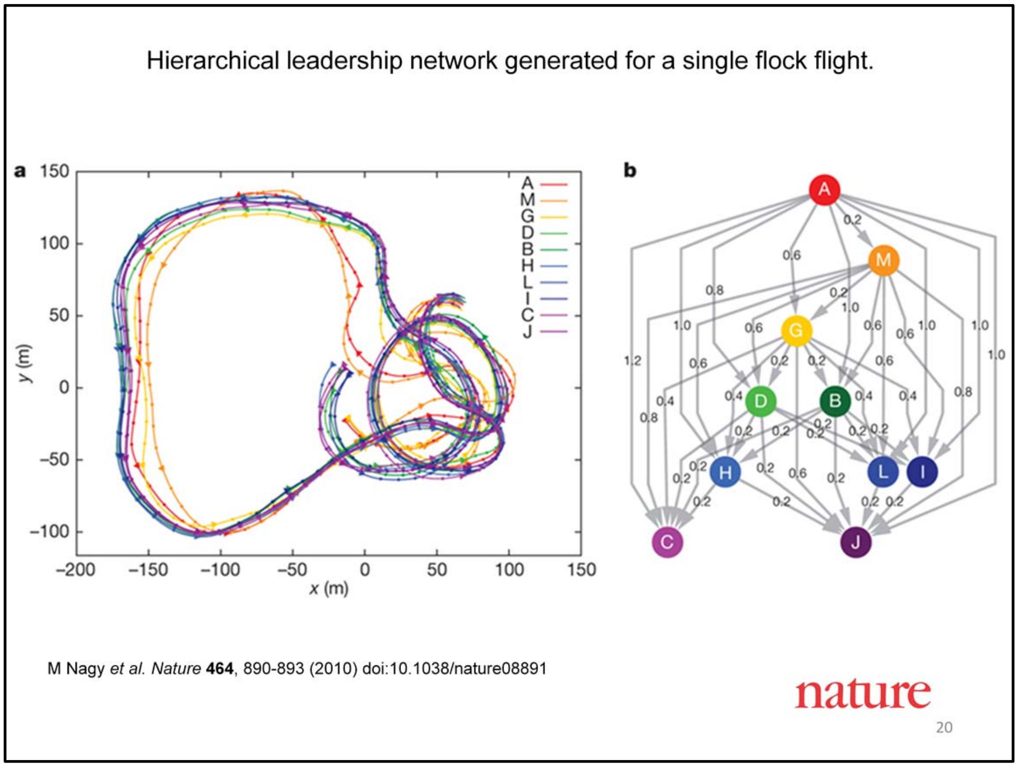

Hierarchical leadership network generated for a single flock flight.

M Nagy *et al. Nature* **464**, 890-893 (2010) doi:10.1038/nature08891

In the work of Nagy et. al. (2010), published in Nature, hierarchies were identified in small flocks of pigeons engaged in (a) free flight as in the picture and (b) homing; video animations will be shown if time permits. The hierarchies were identified by velocity correlations and delays associated to steering actions. For us this data is primarily of interest in illustrating the extraction of kinematic modes.

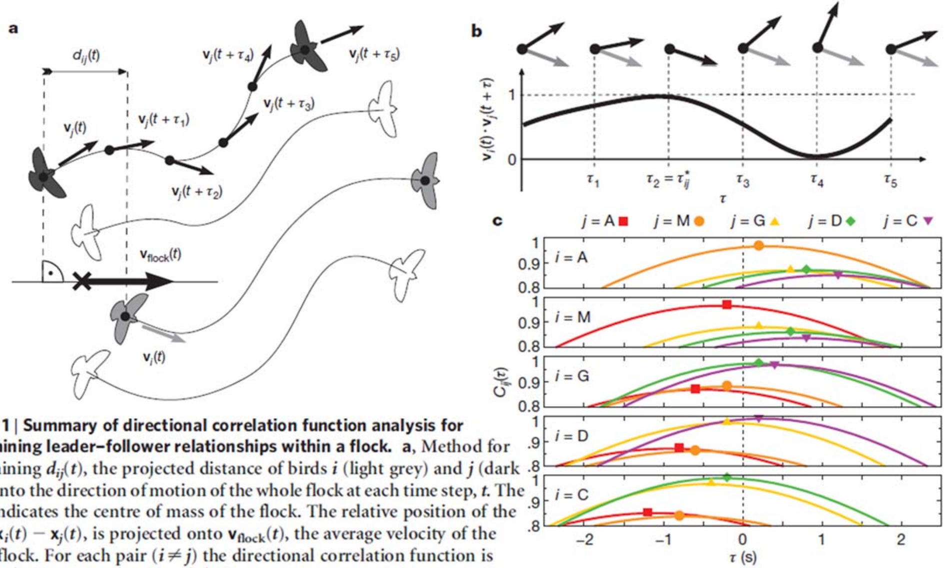

Figure 1 | Summary of directional correlation function analysis for determining leader–follower relationships within a flock. **a**, Method for determining $d_{ij}(t)$, the projected distance of birds i (light grey) and j (dark grey) onto the direction of motion of the whole flock at each time step, t. The cross indicates the centre of mass of the flock. The relative position of the birds, $\mathbf{x}_i(t) - \mathbf{x}_j(t)$, is projected onto $\mathbf{v}_{\mathrm{flock}}(t)$, the average velocity of the whole flock. For each pair ($i \neq j$) the directional correlation function is $C_{ij}(\tau) = \langle \mathbf{v}_i(t) \cdot \mathbf{v}_j(t+\tau) \rangle$, where $\langle ... \rangle$ denotes time average. The arrows show the direction of motion, $\mathbf{v}_i(t)$. **b**, Visualization of the scalar product of the normalized velocity of bird i at time t and that of bird j at time $t+\tau$ in **a**. Here, bird j is following bird i with directional correlation delay time τ^*_{ij}. **c**, $C_{ij}(\tau)$ during a flock flight (that shown in Fig. 2). For more transparency only the data of birds A, M, G, D and C (in the order of hierarchy for that flight) are shown. The solid symbols indicate the maximum value of the correlation function, $C_{ij}(\tau)$.

Hierarchical leadership network generated from multiple flock flights

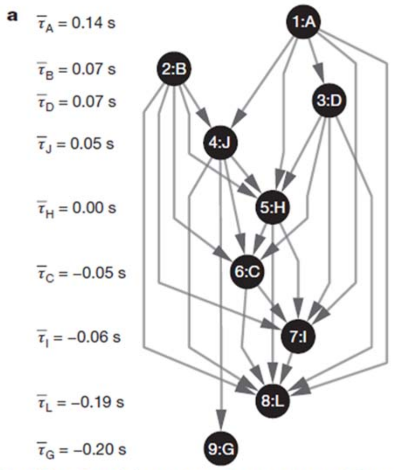

Figure 3 | Hierarchical leadership network generated from multiple flock flights. a, Overall hierarchical network of all birds that flew together on at least two occasions ($C_{\min} = 0.99$). The flock-averaged directional correlation delay time for each bird, $\overline{\tau_i}$, is indicated on the left; note that it has the same order as the network, as it was used to order those birds between whom relative ranks could not be resolved on the basis of edges alone. **b**, Average

M Nagy *et al.* *Nature* **464**, 890-893 (2010) doi:10.1038/nature08891

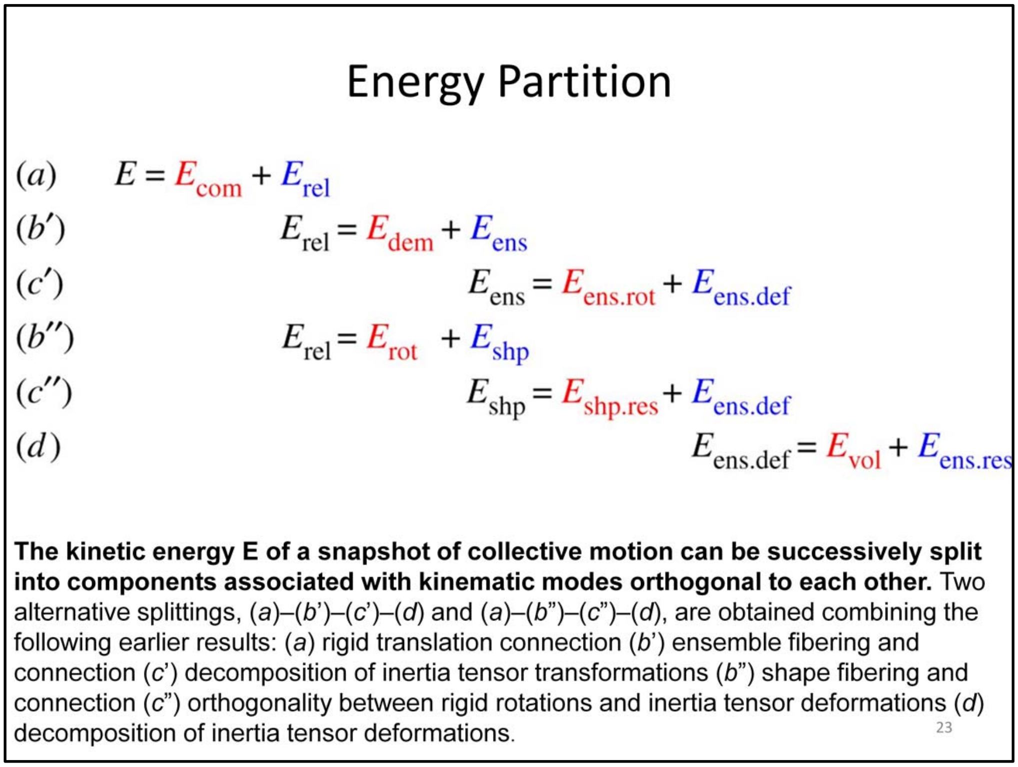

Energy Partition

$$
\begin{array}{ll}
(a) & E = E_{\text{com}} + E_{\text{rel}} \\
(b') & E_{\text{rel}} = E_{\text{dem}} + E_{\text{ens}} \\
(c') & E_{\text{ens}} = E_{\text{ens.rot}} + E_{\text{ens.def}} \\
(b'') & E_{\text{rel}} = E_{\text{rot}} + E_{\text{shp}} \\
(c'') & E_{\text{shp}} = E_{\text{shp.res}} + E_{\text{ens.def}} \\
(d) & E_{\text{ens.def}} = E_{\text{vol}} + E_{\text{ens.res}}
\end{array}
$$

The kinetic energy E of a snapshot of collective motion can be successively split into components associated with kinematic modes orthogonal to each other. Two alternative splittings, (*a*)–(*b*')–(*c*')–(*d*) and (*a*)–(*b*")–(*c*")–(*d*), are obtained combining the following earlier results: (*a*) rigid translation connection (*b*') ensemble fibering and connection (*c*') decomposition of inertia tensor transformations (*b*") shape fibering and connection (*c*") orthogonality between rigid rotations and inertia tensor deformations (*d*) decomposition of inertia tensor deformations.

The kinetic energy *E*($\mathbf{v}_r$) of a snapshot of collective motion vr ∈ TrR can be iteratively split into additive components associated with elementary motions orthogonal to each other. Two alternative splittings, (*a*)–(*b*')–(*c*')–(*d*) and (*a*)–(*b*")–(*c*")–(*d*), are obtained combining the following earlier results: (*a*) rigid translation connection (*b*') ensemble fibering and connection (*c*') decomposition of inertia tensor transformations (*b*") shape fibering and connection (*c*") orthogonality between rigid rotations and inertia tensor deformations (*d*) decomposition of inertia tensor deformations.

We apply this energy partition to the pigeon flock data.

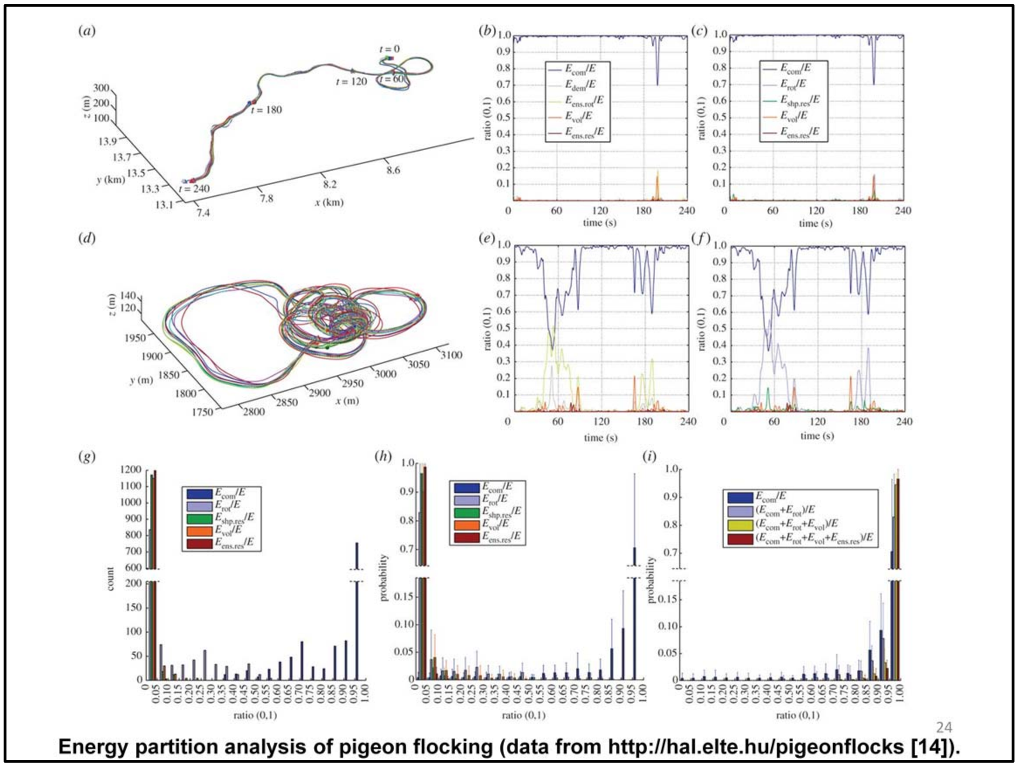

Energy partition analysis of pigeon flocking (data from http://hal.elte.hu/pigeonflocks [14]).

Analysis of pigeon flocking (data from http://hal.elte.hu/pigeonflocks [14]). (*a*) Homing flight trajectories, with time-stamps every 60 s. (*b*,*c*) Time evolution of the energy ratios (6.1)–(6.2) for event (*a*). Note the change around t=200. (*d*–*f*) Free flight trajectories with time evolution of the energy ratios (as in (*a*–*c*)). (*g*) Histogram of the energy ratios (6.2) in (*f*), with split y-axis. Note that E_{rot}/E and E_{vol}/E can be as high as 0.5 and 0.2, respectively. (*h*,*i*) Mean probability distributions across free flights (n=6) of the individual energy ratios ((*h*), consistent with (*g*)) and their cumulative sums (*i*). Error bars denote standard deviation. The sum $(E_{com}+E_{rot}+E_{vol})/E$ has 93±4% probability of being in the range [0.95,1.00] and 4±3% probability of being in the range [0.90,0.95].

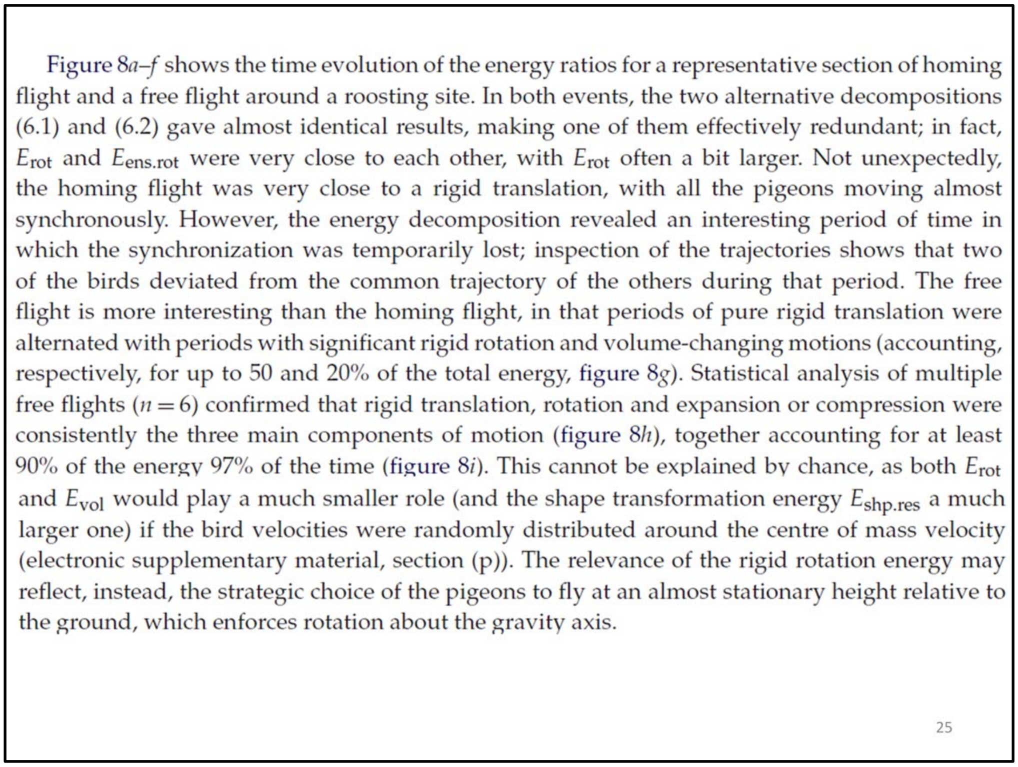

Figure 8*a*–*f* shows the time evolution of the energy ratios for a representative section of homing flight and a free flight around a roosting site. In both events, the two alternative decompositions (6.1) and (6.2) gave almost identical results, making one of them effectively redundant; in fact, E_{rot} and $E_{\mathrm{ens.rot}}$ were very close to each other, with E_{rot} often a bit larger. Not unexpectedly, the homing flight was very close to a rigid translation, with all the pigeons moving almost synchronously. However, the energy decomposition revealed an interesting period of time in which the synchronization was temporarily lost; inspection of the trajectories shows that two of the birds deviated from the common trajectory of the others during that period. The free flight is more interesting than the homing flight, in that periods of pure rigid translation were alternated with periods with significant rigid rotation and volume-changing motions (accounting, respectively, for up to 50 and 20% of the total energy, figure 8*g*). Statistical analysis of multiple free flights ($n = 6$) confirmed that rigid translation, rotation and expansion or compression were consistently the three main components of motion (figure 8*h*), together accounting for at least 90% of the energy 97% of the time (figure 8*i*). This cannot be explained by chance, as both E_{rot} and E_{vol} would play a much smaller role (and the shape transformation energy $E_{\mathrm{shp.res}}$ a much larger one) if the bird velocities were randomly distributed around the centre of mass velocity (electronic supplementary material, section (p)). The relevance of the rigid rotation energy may reflect, instead, the strategic choice of the pigeons to fly at an almost stationary height relative to the ground, which enforces rotation about the gravity axis.

These comments are in reference to the energy partitions of flight data in the previous slide.

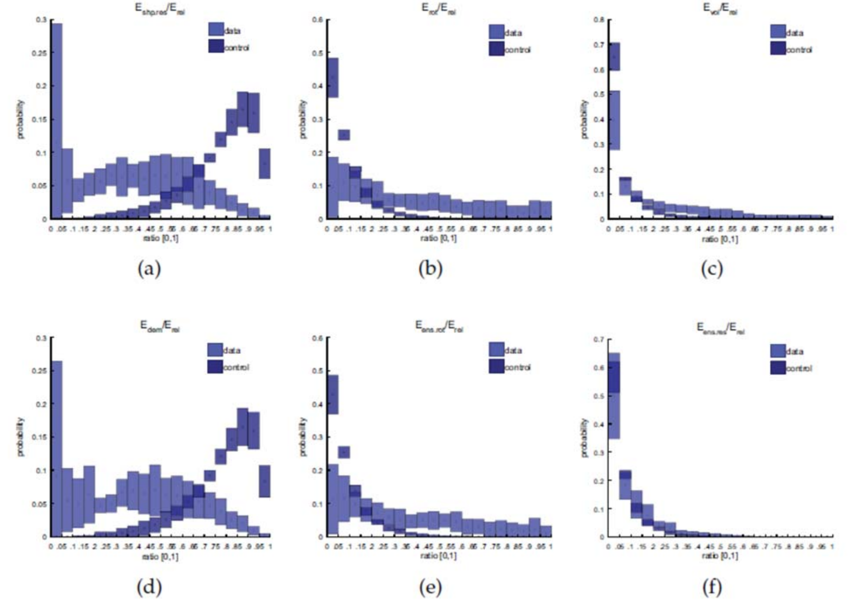

Figure 9. Comparison of mean probability distributions obtained from actual pigeon free flights (*data*, $n = 6$) with those obtained in comparable artificial flocking events generated with random pigeon velocities relative to the center of mass (*control*). All energy ratios are relative to $E_{rel} = E - E_{com}$: (a) $E_{shp.res}/E_{rel}$, (b) E_{rot}/E_{rel}, (c) E_{vol}/E_{rel}, (d) E_{dem}/E_{rel}, (e) $E_{ens.rot}/E_{rel}$, (f) $E_{ens.res}/E_{rel}$. The height of the bars reflects the standard deviation of the distributions ($\pm 1 std$).

References

- Mischiati M, Krishnaprasad PS. 2017 Geometric decompositions of collective motion, *Proc. R. Soc. A* 473:20160571.
- Proccacini A *et. al*. 2011 Propagating waves in starling, *Sturnus vulgaris*, flocks under predation, *Animal Behaviour*, **82**, 759-765.
- Ballerini M *et al.* 2008 Interaction ruling animal collective behavior depends on topological rather than metric distance: evidence from a field study. *Proc. Natl Acad. Sci. USA* **105**, 1232–1237.
- Littlejohn RG, Reinsch M. 1997 Gauge fields in the separation of rotations and internal motions in the n-body problem. *Rev. Mod. Phys.* **69**, 213–275.
- Smale S. 1970 Topology and mechanics. I. *Inventiones math.* **10**, 305–331.
- Hausmann J-C, Knutson A. 1997 Polygon spaces and Grassmannians. *L'Enseignement Mathematique* **43**, 173–198.
- Nagy M, Akos Z, Biro D, Vicsek T. 2010 Hierarchical group dynamics in pigeon flocks. *Nature,* **464**, 890–894.

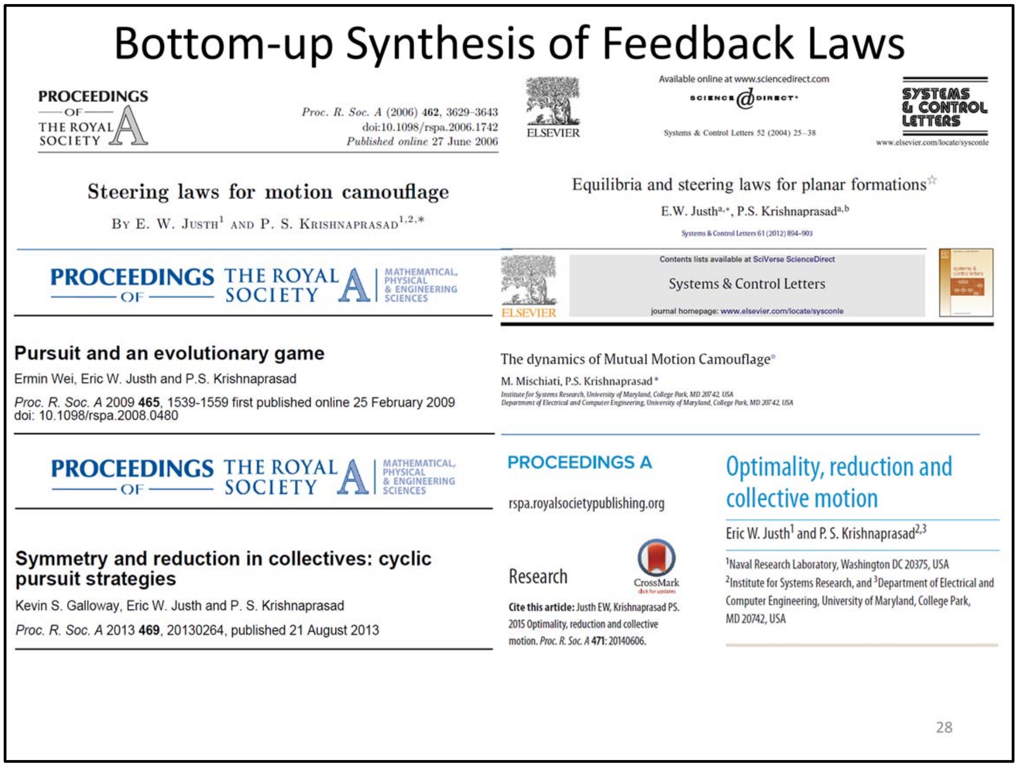

Bottom-up Synthesis of Feedback Laws

PROCEEDINGS
OF
THE ROYAL
SOCIETY A

Proc. R. Soc. A (2006) **462**, 3629–3643
doi:10.1098/rspa.2006.1742
Published online 27 June 2006

Steering laws for motion camouflage

By E. W. Justh[1] and P. S. Krishnaprasad[1,2,*]

PROCEEDINGS OF THE ROYAL SOCIETY A MATHEMATICAL, PHYSICAL & ENGINEERING SCIENCES

Pursuit and an evolutionary game

Ermin Wei, Eric W. Justh and P.S. Krishnaprasad

Proc. R. Soc. A 2009 **465**, 1539-1559 first published online 25 February 2009
doi: 10.1098/rspa.2008.0480

PROCEEDINGS OF THE ROYAL SOCIETY A MATHEMATICAL, PHYSICAL & ENGINEERING SCIENCES

Symmetry and reduction in collectives: cyclic pursuit strategies

Kevin S. Galloway, Eric W. Justh and P. S. Krishnaprasad

Proc. R. Soc. A 2013 **469**, 20130264, published 21 August 2013

ELSEVIER

Available online at www.sciencedirect.com
SCIENCE DIRECT

Systems & Control Letters 52 (2004) 25–38

SYSTEMS & CONTROL LETTERS
www.elsevier.com/locate/sysconle

Equilibria and steering laws for planar formations☆

E.W. Justh[a,*], P.S. Krishnaprasad[a,b]

Systems & Control Letters 61 (2012) 894–903

ELSEVIER

Contents lists available at SciVerse ScienceDirect

Systems & Control Letters

journal homepage: www.elsevier.com/locate/sysconle

The dynamics of Mutual Motion Camouflage☆

M. Mischiati, P.S. Krishnaprasad *

Institute for Systems Research, University of Maryland, College Park, MD 20742, USA
Department of Electrical and Computer Engineering, University of Maryland, College Park, MD 20742, USA

PROCEEDINGS A

rspa.royalsocietypublishing.org

Research

CrossMark

Cite this article: Justh EW, Krishnaprasad PS. 2015 Optimality, reduction and collective motion. *Proc. R. Soc. A* **471**: 20140606.

Optimality, reduction and collective motion

Eric W. Justh[1] and P. S. Krishnaprasad[2,3]

[1]Naval Research Laboratory, Washington DC 20375, USA
[2]Institute for Systems Research, and [3]Department of Electrical and Computer Engineering, University of Maryland, College Park, MD 20742, USA

Prior work on dyadic and polyadic interactions (between agents modeled as active particles), developed bio-inspired sensori-motor feedback laws as building blocks for collective behavior. We also examined interactions derived from optimal control principles applied to collective cost functionals. Graph-based descriptions – such as cyclic pursuit strategies, were used in bottom-up synthesis techniques, and analyzed by symmetry reduction to shape spaces and applications of dynamical systems principles. We aim to bring together these results and the data representations (modes) discussed today to solve the inverse problem of uncovering mechanisms of natural collective behavior.

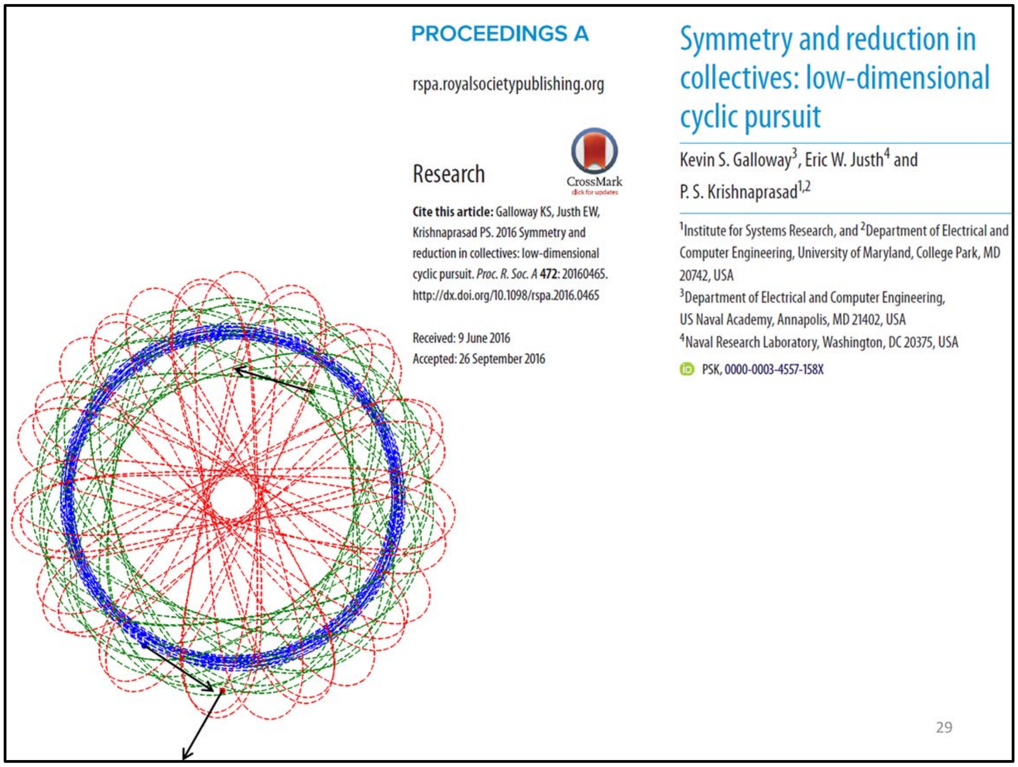

PROCEEDINGS A

rspa.royalsocietypublishing.org

Research

Cite this article: Galloway KS, Justh EW, Krishnaprasad PS. 2016 Symmetry and reduction in collectives: low-dimensional cyclic pursuit. *Proc. R. Soc. A* **472**: 20160465. http://dx.doi.org/10.1098/rspa.2016.0465

Received: 9 June 2016
Accepted: 26 September 2016

Symmetry and reduction in collectives: low-dimensional cyclic pursuit

Kevin S. Galloway[3], Eric W. Justh[4] and P. S. Krishnaprasad[1,2]

[1]Institute for Systems Research, and [2]Department of Electrical and Computer Engineering, University of Maryland, College Park, MD 20742, USA
[3]Department of Electrical and Computer Engineering, US Naval Academy, Annapolis, MD 21402, USA
[4]Naval Research Laboratory, Washington, DC 20375, USA

PSK, 0000-0003-4557-158X

29

In the setting of 3 agent constant bearing cyclic pursuit, there arise parameter values supporting periodic orbits in phase space (reduced from 9 dimensions to 2 dimensions by SE(2) symmetry, restriction to attracting invariant manifold, and change of time scale). The arguments use time-reversal symmetry. Figure shows physical space trajectories.

Such low dimensional examples may arise as **motifs** with interesting dynamical aspects that influence overall complex flock behavior.

Thank you for listening